

New limits from lepton flavour violating processes on the Littlest Higgs model with T-parity

I. Pacheco and P. Roig

Departamento de Física, Centro de Investigación y de Estudios Avanzados del Instituto Politécnico Nacional, Apartado Postal 14-740, 07000 Ciudad de México, México.

Received 30 October 2021; accepted 3 December 2021

We study lepton flavor violation (LFV) within the Littlest Higgs Model with T parity (LHT) realizing an inverse seesaw (ISS) mechanism of type I. In this scenario there appear new \mathcal{O} (TeV) Majorana neutrinos, driving LFV. We analyze the heavy Majorana neutrinos effects on LFV processes: $\ell \rightarrow \ell' \gamma$, $Z \rightarrow \bar{\ell} \ell'$, $L \rightarrow 3\ell$ decays and $\mu \rightarrow e$ conversion in nuclei, but we emphasize Type III decay channel of $L \rightarrow 3\ell$ which are known as “wrong-sign”: $\ell \rightarrow \ell' \ell'' \ell'''$ satisfying $\ell \neq \ell' = \ell'' \neq \ell'''$, since these processes vanish in the traditional LHT. First, we obtain limits to $|\theta_{e j} \theta_{\mu j}^\dagger|$, $|\theta_{e j} \theta_{\tau j}^\dagger|$, and $|\theta_{\mu j} \theta_{\tau j}^\dagger|$ through $\ell \rightarrow \ell' \gamma$. Using these limits for the product of the mixing angles, we can demonstrate that results for branching ratios of wrong-sign processes yield within one order of magnitude below present bounds. We do not expect large correlations between the two wrong-sign decay modes. Also, we see that the mean values of heavy Majorana neutrino masses for all LFV processes are quasi-degenerate around 4 TeV [1].

Keywords: Discrete symmetries; beyond standard model; technicolor and composite models.

DOI: <https://doi.org/10.31349/SuplRevMexFis.3.020704>

1. Introduction

Despite SM is a theory which describes all known elementary particles processes successfully, it has a severe problem due to the Higgs mass-squared receives quadratically divergent radiative corrections coming from the interactions with SM fields. Over time several models have been proposed trying to solve this problem. Little Higgs models [2, 3] offer an explanation to the little hierarchy between the Higgs mass M_h assumed to be near the electroweak scale $v = 246$ GeV and the new physics (NP) scale f , whose value is expected to be ~ 1 TeV [4–6]. In this set of models, the Higgs boson is originated as a pseudo-Nambu-Goldstone boson (pNGB) of a spontaneously broken global symmetry. Specifically, the Littlest Higgs model with T parity (LHT) [2, 3, 7–11] is one of the most attractive such frameworks. LHT is based on the coset space $SU(5)/SO(5)$, where $SU(5)$ is the global symmetry broken by a vacuum expectation value (vev) at a scale of few TeV. The vev is represented by a 5×5 symmetric tensor [12, 13]

$$\Sigma_0 = \begin{pmatrix} 0 & 0 & \mathbb{I} \\ 0 & 1 & 0 \\ \mathbb{I} & 0 & 0 \end{pmatrix}. \quad (1)$$

As $SU(5)$ has 24 generators, after symmetry breaking, the 10 unbroken $SO(5)$ generators satisfy

$$T_a \Sigma_0 + \Sigma_0 T_a^T = 0, \quad (2)$$

whereas the 14 broken generators obey

$$X_a \Sigma_0 - \Sigma_0 X_a^T = 0. \quad (3)$$

Goldstone bosons are fluctuations around this background in the broken directions $\Pi \equiv \pi^a \hat{X}^a$, and can be parameterized by the non-linear sigma model field

$$\Sigma(x) = e^{i\Pi/f} \Sigma_0 e^{i\Pi^T/f} = e^{2i\Pi/f} \Sigma_0, \quad (4)$$

where f is the NP energy scale. Thus the matrix of NGB can be written as [12, 14]

$$\Pi = \begin{pmatrix} \chi + \frac{\eta}{2\sqrt{5}} & \frac{h}{\sqrt{2}} & \phi \\ \frac{h^\dagger}{\sqrt{2}} & \frac{2\eta}{\sqrt{5}} & \frac{h^T}{\sqrt{2}} \\ \phi^\dagger & \frac{h^*}{\sqrt{2}} & \chi^T + \frac{\eta}{2\sqrt{5}} \end{pmatrix}. \quad (5)$$

The content of NGB is as follows: ϕ is a complex $SU(2)_L$ triplet; χ and η are the Goldstone bosons which become the longitudinal modes of the T-odd gauge fields. They are written explicitly as

$$\phi = \begin{pmatrix} -i\Phi^{++} & -i\frac{\Phi^+}{\sqrt{2}} \\ -i\frac{\Phi^+}{\sqrt{2}} & -\frac{\Phi^0 + \Phi^P}{\sqrt{2}} \end{pmatrix}, \quad (6)$$

$$\chi = \begin{pmatrix} -\omega^0/2 & -\omega^+/\sqrt{2} \\ -\omega^-/\sqrt{2} & \omega^0/2 \end{pmatrix}, \quad (7)$$

so, the fields ω^\pm , ω^0 and η are eaten by the heavy gauge bosons W_H^\pm , Z_H and A_H , respectively. h is the SM Higgs doublet

$$h = \begin{pmatrix} -i\pi^+/\sqrt{2} \\ \frac{v+h+i\pi^0}{2} \end{pmatrix}. \quad (8)$$

The discrete T-parity symmetry is a Z_2 one (similar to R-parity in SUSY), where SM particles are even under it (T-even), while the new particles at the TeV scale are odd (T-odd). T-parity forbids singly-produced heavy particles (odd under T) and tree level corrections to observables with only SM particles. As a result, direct and indirect constraints on the LHT are significantly relaxed [14, 15], and corrections to EWPO are generated at loop level. Thus, the LHT remains phenomenologically viable [12, 16–37].

LHT belongs the Product Group models, so the gauge group is taken to be $G_1 \times G_2 = [SU(2) \times U(1)]^2$, subgroup of the $SU(5)$ global symmetry. A natural action of T-parity on the gauge fields is defined as

$$G_1 \leftrightarrow G_2. \quad (9)$$

In the gauge sector before EWSB, the SM (light) gauge bosons are W_L^a and B_L which are massless and T-even, while the massive heavy gauge bosons (T-odd) are W_H^a and B_H . After high energy symmetry breaking, their masses are [15]

$$M_{W_H^a} = g_W f, \quad M_{B_H} = \frac{g' f}{\sqrt{5}}, \quad (10)$$

where $e = g_W s_W = g' c_W$.

When EWSB is included, the masses of SM bosons are given by [12, 15]

$$\begin{aligned} M_{W_L^\pm} &= \frac{g_W v}{2} \left(1 - \frac{v^2}{6f^2}\right)^{1/2} \approx \frac{g_W v}{2} \left(1 - \frac{v^2}{12f^2}\right), \\ M_{Z_L} &= \frac{g_W v}{2 \cos \theta_H} \left(1 - \frac{v^2}{6f^2}\right)^{1/2} = \frac{M_{W_L^\pm}}{\cos \theta_H}, \\ M_{A_L} &= 0. \end{aligned} \quad (11)$$

It is important to observe that ρ factor is conserved in LHT in contrast to SLH, since in the latter model ρ has corrections of the order of v^2/f^2 .

In the heavy sector the masses are written as follows [12, 15]

$$\begin{aligned} M_{W_H^\pm} &= M_{Z_H} = f g_W \left(1 - \frac{v^2}{4f^2}\right)^{1/2} \approx f g_W \left(1 - \frac{v^2}{8f^2}\right), \\ M_{A_H} &= \frac{f g'}{\sqrt{5}} \left(1 - \frac{5v^2}{4f^2}\right)^{1/2} \approx \frac{f g'}{\sqrt{5}} \left(1 - \frac{5v^2}{8f^2}\right). \end{aligned} \quad (12)$$

Including fermion sector is less straightforward than scalar one. For each SM lepton doublet, two doublets ψ_1 and ψ_2 are introduced by an incomplete representation $\Psi_1, \Psi_2 \in SU(5)$ symmetry. The field content can be expressed as follows (σ^2 is the second Pauli matrix)

$$\begin{aligned} \Psi_1 &= \begin{pmatrix} \psi_1 \\ 0 \\ 0 \end{pmatrix}, \quad \Psi_2 = \begin{pmatrix} 0 \\ 0 \\ \psi_2 \end{pmatrix}, \\ \psi_i &= -i\sigma^2 \begin{pmatrix} \nu_{iL} \\ \ell_{iL} \end{pmatrix}, \end{aligned} \quad (13)$$

with $i = 1, 2$, where Ψ_2 transforms with the fundamental $SU(5)$ representation \mathbf{V} and Ψ_1 with its complex conjugated. T-parity is defined to act on the left-handed (LH) leptons as

$$\Psi_1 \longleftrightarrow \Omega \Sigma_0 \Psi_2, \quad (14)$$

with

$$\begin{aligned} \Omega &= \text{diag}(-1, -1, 1, -1, -1), \\ \Sigma_0 &= \begin{pmatrix} 0 & 0 & \mathbf{1}_{2 \times 2} \\ 0 & 1 & 0 \\ \mathbf{1}_{2 \times 2} & 0 & 0 \end{pmatrix}. \end{aligned} \quad (15)$$

The T-even combination of ψ_1 and ψ_2 will be identified as the SM electroweak leptons

$$\psi_{SM} = \frac{1}{\sqrt{2}} (\psi_1 - \psi_2), \quad (16)$$

which receives mass after EWSB from Yukawa interactions, while T-odd combination, defined as follows

$$\psi_{HL} = \frac{1}{\sqrt{2}} (\psi_1 + \psi_2), \quad (17)$$

refers to a Dirac mass of order $\mathcal{O}(f)$. This heavy eigenstate gets its mass combining with an additional set of fermions in a T-odd $SO(5)$ multiplet Ψ_R^c , which is right-handed

$$\Psi_R = \begin{pmatrix} \psi_R^c \\ \chi_R \\ \psi_{HR} \end{pmatrix} \quad T : \Psi_R \leftrightarrow \Omega \Psi_R. \quad (18)$$

It is important that Yukawa Lagrangian be invariant under $SU(5)$ and T-parity, thus with aid of $\xi = \exp(i\Pi/f)$ field, it will be written

$$\begin{aligned} \mathcal{L}_{Y_H} &= \kappa_1 f (\bar{\Psi}_2 \xi + \bar{\Psi}_1 \Sigma_0 \xi^\dagger) \Psi_R \\ &= \sqrt{2} \kappa_1 f \bar{\psi}_{HL} \psi_{HR} + \dots \end{aligned} \quad (19)$$

We see that T-odd combination receives a Dirac mass $M_- = \sqrt{2} \kappa_1 f$, whereas the T-even combination ψ_{SM} remains massless, as we expected. After EWSB, a small mass splitting between the T-odd leptons and neutrinos is induced at order of $\mathcal{O}(v^2/f^2)$, becoming

$$m_{\nu_H} = \sqrt{2} \kappa_1 f \left(1 - \frac{v^2}{8f^2}\right), \quad m_{\ell_H} = \sqrt{2} \kappa_1 f. \quad (20)$$

2. New contributions to LFV processes

As we know, the SM contributions to the LFV processes like $\mu \rightarrow e\gamma$ and $\mu \rightarrow ee\bar{e}$ are negligible since they are proportional to the neutrino masses. Nevertheless, we expect that LHT contributions have a sizeable effect in LFV due to the exchange of the new vector bosons and heavy fermions coming from the T-parity.

Two types of diagrams contribute to $\ell \rightarrow \ell' \ell'' \ell'''$, which are shown in Fig. 1.

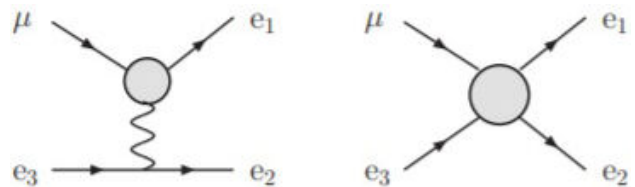
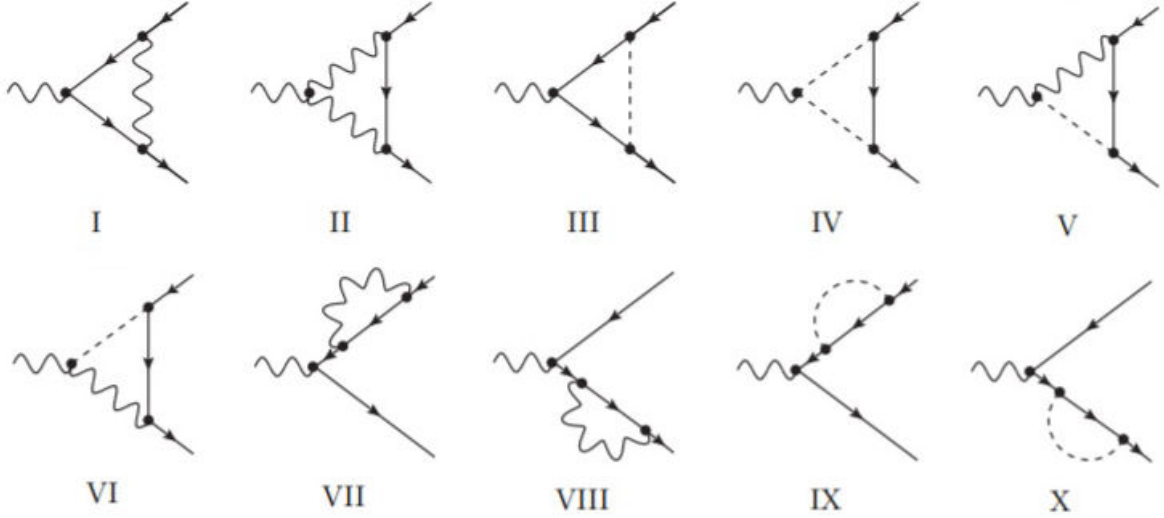


FIGURE 1. Generic penguin and box diagrams for $\mu \rightarrow ee\bar{e}$.

FIGURE 2. Topologies of the diagrams that contribute to two and three-body lepton decays as well as $\gamma, Z \rightarrow \bar{\ell}\ell'$.

3. Extracting form factors from the $\ell \rightarrow \ell'\gamma$ amplitude

Most general structure of the $\ell \rightarrow \ell'\gamma$ effective vertex can be expressed in terms of six form factors

$$i\Gamma^\mu(p_1, p_2) = ie \left[\gamma^\mu (F_L^V P_L + F_R^V P_R) + (iF_M^V + F_E^V \gamma_5) \sigma^{\mu\nu} Q_\nu + (iF_S^V + F_P^V \gamma_5) Q^\mu \right], \quad (21)$$

with $Q = p_2 - p_1$ the vector boson momentum entering the vertex. Under the consideration that the photon is on-shell, only the dipole form factors $F_{M,E}^\gamma$ contribute.

In Fig. 2 we show the topologies of the diagrams that contribute to the $V - \bar{\ell} - \ell'$ ($V = \gamma/Z$) effective vertex.

The form factor F_M^γ is given by the contributions [35]

$$F_M^\gamma = F_M^\gamma|_{W_H} + F_M^\gamma|_{Z_H} + F_M^\gamma|_{A_H} + F_M^\gamma|_{\bar{\nu}^c} + F_M^\gamma|_{\bar{\ell}^c}. \quad (22)$$

There are two additional contributions coming from the exclusive fermion content of LHT (they had not been considered until [35]). The contributions from partner leptons $\bar{\ell}^c = (\bar{\nu}^c, \bar{\ell}^c)$ only involve topologies III, IV, IX and X (see Fig. 2), because they do not couple to one T-odd gauge boson and a SM charged lepton. We computed all form factors with aid of Package-X [41]. Then, neglecting $m_{\ell'} \ll m_\ell$,

$$\Gamma(\ell \rightarrow \ell'\gamma) = \frac{\alpha}{2} m_\ell^3 (|F_M^\gamma|^2 + |F_E^\gamma|^2). \quad (23)$$

4. Extracting form factors from the $\mu \rightarrow ee\bar{e}$ amplitude

This process can be studied like a $\ell \rightarrow \ell'\bar{\ell}'\ell'$ decay which involves photon and Z penguin diagrams as well as box contributions.

The effective vertex reads as follows

$$i\Gamma_\gamma^\mu(p_\ell, p_{\ell'}) = ie \left\{ [iF_M^\gamma(Q^2) + F_E^\gamma(Q^2)\gamma_5] \sigma^{\mu\nu} Q_\nu + F_L^\gamma(Q^2)\gamma^\mu P_L \right\}, \quad (24)$$

with $Q_\nu = (p_{\ell'} - p_\ell)_\nu$. In our case $\ell \rightarrow \mu$ and $\ell' \rightarrow e$, therefore the corresponding right-handed vector form factor vanishes ($m_e \approx 0$). Due to the constraints of LHT only photon and Z penguin diagrams contribute, since A_H and Z_H do not couple to two SM fermions.

In the γ -penguin contribution the F_M^γ and F_E^γ form factors have the same expressions as Eq. (22). For an on-shell photon, terms proportional to Q^2 vanish. Hence, the F_L^γ form factor receives the following contributions [35]

$$F_L^\gamma = F_L^\gamma|_{W_H} + F_L^\gamma|_{Z_H} + F_L^\gamma|_{A_H} + F_L^\gamma|_{\bar{\nu}^c} + F_L^\gamma|_{\bar{\ell}^c}. \quad (25)$$

In the Z -penguin contributions the dipole form factors $F_{M,E}^Z$, which are chirality flipping and hence proportional to the muon mass, vanish when they are compared to F_L^Z . Thus, at leading order the $Z\bar{\ell}\ell'$ vertex reduces to

$$i\Gamma_Z^\mu(p_\ell, p_{\ell'}) = ie F_L^Z(Q^2)\gamma^\mu P_L, \quad (26)$$

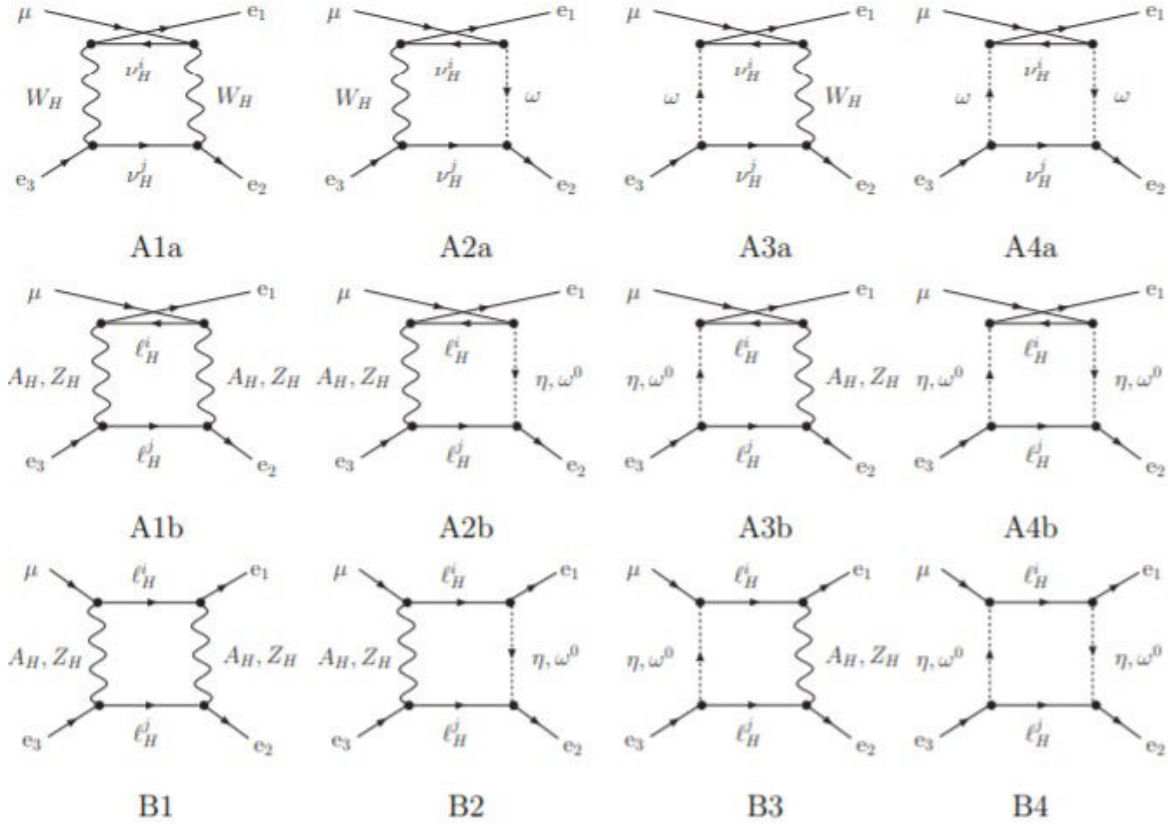
where we obtain [35]

$$F_L^Z = F_L^Z|_{W_H} + F_L^Z|_{A_H} + F_L^Z|_{Z_H} + F_L^Z|_{\bar{\nu}^c} + F_L^Z|_{\bar{\ell}^c}. \quad (27)$$

The amplitude due to box diagrams is given by

$$\mathcal{M}_{\text{box}}^{\ell \rightarrow \ell' \bar{\ell}' \ell'} = e^2 B_L(0) \bar{u}(p_1) \gamma^\mu \times P_L u(p_\ell) \bar{u}(p_3) \gamma_\mu P_L v(p_2). \quad (28)$$

Figure 3 shows the box diagrams contributing to $\mu \rightarrow ee\bar{e}$ decay. The whole $B_L(0)$ form factor receives the following contributions [35]

FIGURE 3. Box diagrams corresponding to $\mu \rightarrow ee\bar{e}$ process in the LHT model.

$$B_L(0) = B_L(W_H, W_H) + B_L(Z_H, Z_H) + B_L(A_H, A_H) + B_L(A_H, Z_H) + B_L(\Phi, \Phi). \quad (29)$$

We expect the new interactions that appear from the heavy particles (T-odd) to contribute sizeably to LFV processes called “wrong sign”: $\ell \rightarrow \ell' \ell'' \bar{\ell}'''$ with $\ell \neq \ell' = \ell'' \neq \ell'''$. We can see in Table I limits on LFV processes presented in Ref. [35] where they are mediated by SM gauge boson and Higgs.

When LHT effects are included the branching ratios become [35]

TABLE I. Experimental upper limits on the $L \rightarrow 3\ell$ LFV processes.

Branching Ratio	90% C.L. Bound
$\tau \rightarrow \mu \bar{e} \mu$	1.7×10^{-8}
$\tau \rightarrow e \bar{\mu} e$	1.5×10^{-8}
$\tau \rightarrow \mu \bar{e} e$	1.8×10^{-8}
$\tau \rightarrow e \bar{\mu} \mu$	2.7×10^{-8}
$\tau \rightarrow e \bar{e} e$	2.7×10^{-8}
$\tau \rightarrow \mu \bar{\mu} \mu$	2.1×10^{-8}

TABLE II. Contributions come from LHT due to T-odd leptons.

Process	Branching Ratio
$\tau \rightarrow \mu \bar{e} \mu$	0
$\tau \rightarrow e \bar{\mu} e$	0
$\tau \rightarrow \mu \bar{e} e$	8.2×10^{-12}
$\tau \rightarrow e \bar{\mu} \mu$	2.2×10^{-12}
$\tau \rightarrow e \bar{e} e$	7.4×10^{-12}
$\tau \rightarrow \mu \bar{\mu} \mu$	1.4×10^{-12}

As we can observe the branching ratios of the wrong sign processes vanish. In the following sections we consider Majorana neutrinos in LHT for computing wrong sign processes in order to get non zero results, since it is known that the heavy Majorana masses (in the TeV scale) impact LFV processes [38–40].

5. Inverse seesaw neutrino masses in the LHT model

We do an extension of LHT model implementing Majorana neutrinos with an ISS mechanism, you can see more details of this method in [36], the main aspects are shown next.

We need to recall that Yukawa Lagrangian (see Eq. (19)) gives masses at order of $\sim f$, it is written as [12, 36]

$$\begin{aligned}\mathcal{L}_{YH} &= \kappa_1 f (\bar{\Psi}_2 \xi + \bar{\Psi}_1 \Sigma_0 \xi^\dagger) \Psi_R \\ &= \sqrt{2} \kappa_1 f \bar{\psi}_{HL} \psi_{HR} + \dots,\end{aligned}\quad (30)$$

where we have approximated $\xi = \exp(i\Pi/f) \approx \mathbb{1}$.

Symmetry allows us to introduce a lepton singlet χ_L , which gets mass by combining directly with a RH singlet χ_R through a direct mass term. Thus, its mass term is read

$$\mathcal{L}_M = -M \bar{\chi}_L \chi_R + h.c.. \quad (31)$$

Since χ_L is a $SU(5)$ singlet we can include a small Majorana mass for it. We assume LN to be broken by small Majorana masses μ in the heavy LH neutral sector, then

$$\mathcal{L}_\mu = -\frac{\mu}{2} \bar{\chi}_L^c \chi_L + h.c.. \quad (32)$$

The neutrino mass matrix, which must be T-even, reduces to the inverse see-saw one [36]

$$\mathcal{L}_M^\nu = -\frac{1}{2} (\bar{\nu}_l^c \bar{\chi}_R \bar{\chi}_L^c) \mathcal{M}_\nu^{T\text{-even}} \begin{pmatrix} \nu_L \\ \chi_R^c \\ \chi_L \end{pmatrix} + h.c., \quad (33)$$

where

$$\mathcal{M}_\nu^{T\text{-even}} = \begin{pmatrix} 0 & i\kappa^* f \sin\left(\frac{v}{\sqrt{2}f}\right) & 0 \\ i\kappa^\dagger f \sin\left(\frac{v}{\sqrt{2}f}\right) & 0 & M^\dagger \\ 0 & M^* & \mu \end{pmatrix}. \quad (34)$$

We recall the ISS hierarchy $\mu \ll \kappa \ll M$. The mass eigenvalues for M are ~ 10 TeV, of the order of $4\pi f$ with $f \sim$ TeV, if we assume the κ eigenvalues to be order 1. While the μ eigenvalues are smaller than the GeV.

The mass eigenstates from Eq. (34) are given by

$$\begin{aligned}\sum_{j=1}^3 U_{ij} \nu_{Lj}^l &= \sum_{j=1}^3 \left(\mathbf{1}_{3\times 3} - \frac{1}{2} [\theta\theta^\dagger] \right)_{ij} \nu_{Lj} - \sum_{j=7}^9 \theta_{ij} \chi_{Lj}, \\ \chi_{Li}^h &= \sum_{j=7}^9 \left(\mathbf{1}_{3\times 3} - \frac{1}{2} [\theta^\dagger\theta] \right)_{ij} \chi_{Lj} + \sum_{j=1}^3 \theta_{ij}^\dagger \nu_{Lj},\end{aligned}\quad (35)$$

where

$$\theta = -if \sin\left(\frac{v}{\sqrt{2}f}\right) \kappa M^{-1}, \quad (36)$$

with U denoting the U_{PMNS} matrix. Therefore, the mass matrix \mathcal{M}_ν^l for light (active) neutrinos is

$$(\mathcal{M}_\nu^l)_{ij} = \theta_{ik}^* \mu_{kl} \theta_{jl}^\dagger. \quad (37)$$

In terms of the mass eigenstates the SM charged currents are modified as follows

$$\begin{aligned}\mathcal{L}_W^l &= \frac{g}{\sqrt{2}} W_\mu^+ \sum_{j=1}^3 \sum_{i=1}^3 \bar{\nu}_i^l W_{ij} \gamma^\mu P_L \ell_j + h.c., \\ \mathcal{L}_W^{lh} &= \frac{g}{\sqrt{2}} W_\mu^+ \sum_{j=1}^3 \sum_{i=7}^9 \bar{\chi}_i^h \theta_{ij}^\dagger \gamma^\mu P_L \ell_j + h.c..\end{aligned}\quad (38)$$

where W matrix has been defined as

$$W_{ij} = \{U^\dagger [\mathbf{1}_{3\times 3} - \frac{1}{2}(\Theta\Theta^\dagger)]\}_{ij}. \quad (39)$$

And the SM neutral currents become

$$\begin{aligned}\mathcal{L}_Z^l &= \frac{g}{2 \cos \theta_W} Z_\mu \sum_{i,j=1}^3 \bar{\nu}_i^l \gamma^\mu (X_{ij} P_L - X_{ij}^\dagger P_R) \nu_j^l, \\ \mathcal{L}_Z^{lh} &= \frac{g}{2 \cos \theta_W} Z_\mu \sum_{i,j=1}^3 \bar{\chi}_i^h \gamma^\mu (Y_{ij} P_L - Y_{ij}^\dagger P_R) \nu_j^l + h.c., \\ \mathcal{L}_Z^h &= \frac{g}{2 \cos \theta_W} Z_\mu \sum_{i,j=1}^3 \bar{\chi}_i^h \gamma^\mu (S_{ij} P_L - S_{ij}^\dagger P_R) \chi_j^h,\end{aligned}\quad (40)$$

whose neutral couplings turn out to be

$$\begin{aligned}X_{ij} &= \sum_{k=1}^3 (U^\dagger [\mathbf{1}_{3\times 3} - (\theta\theta^\dagger)])_{ik} U_{kj}, \\ Y_{ij} &= \sum_{k=1}^3 \theta_{ik}^\dagger U_{kj}, \quad S_{ij} = \sum_{k=1}^3 \theta_{ik}^\dagger \theta_{kj}.\end{aligned}\quad (41)$$

If we compare our charged-current and neutral-current interactions with the SM ones, we observe that they differ by the presence of the θ matrix which is consequence of introducing Majorana neutrinos.

6. Bounds on LFV processes

Along the calculation we will use 't Hooft-Feynman gauge. We present two types of LFV processes in this section: $\ell \rightarrow \ell' \gamma$ and $\ell \rightarrow \ell' \ell'' \ell'''$, where the last one has three possible channels but we are just focusing on wrong sign processes ($\ell \neq \ell' = \ell'' \neq \ell'''$) involving Majorana Neutrinos.

6.1. $\ell \rightarrow \ell' \gamma$ decays

From Eq. (23) and using $F_M^\gamma = -iF_E^\gamma$ the results will be simplified. The contribution coming from light and heavy Majorana neutrinos is

$$\begin{aligned}\text{Br}(\mu \rightarrow e \gamma) &= \frac{3\alpha}{2\pi} \left| W_{e\mu} W_{\mu e}^* F_M^\chi(x_j) \right. \\ &\quad \left. + U_{e\mu} U_{\mu e}^* F_M^\nu(y_i) \right|^2,\end{aligned}\quad (42)$$

recalling that $U = U_{\text{PMNS}}$ and W is given by Eq. (39). For active neutrinos ($m_{\nu_i} \ll M_W$), the $F_M^\nu(y)$ function, defining $y = m_{\nu_i}^2/M_W^2$, yields

$$F_M^\nu(y) = \frac{5}{6} - \frac{3y - 15y^2 - 6y^3}{12(1-y)^3} + \frac{3y^3}{2(1-y)^4} \ln y, \quad (43)$$

and for heavy neutrinos ($m_{\chi_i^h} \gg M_W$)

$$F_M^X(x) = \frac{1}{3} - \frac{2x^3 - 7x^2 + 11x}{4(1-x)^3} + \frac{3x}{2(1-x)^4} \ln x, \quad (44)$$

with $x = M_W^2/m_{\chi_h}^2$, being m_{χ_h} the mass of heavy Majorana neutrinos.

The branching ratio for $\mu \rightarrow e\gamma$ turns out to be

$$\text{Br}(\mu \rightarrow e\gamma) \approx \frac{3\alpha}{8\pi} \left| \theta_{ej} \theta_{\mu j}^\dagger \right|^2. \quad (45)$$

By considering the general form for the $\ell \rightarrow \ell'\gamma$ decays we do the proper replacements on the Eq. (45). Then, the 90% C.L. limits $\text{Br}(\mu \rightarrow e\gamma) < 4.2 \times 10^{-13}$, $\text{Br}(\tau \rightarrow e\gamma) < 3.3 \times 10^{-8}$ and $\text{Br}(\tau \rightarrow \mu\gamma) < 4.2 \times 10^{-8}$ [42, 43] bind

$$\begin{aligned} |\theta_{ej} \theta_{\mu j}^\dagger| &< 0.14 \times 10^{-4}, & |\theta_{ej} \theta_{\tau j}^\dagger| &< 0.95 \times 10^{-2}, \\ |\theta_{\mu j} \theta_{\tau j}^\dagger| &< 0.011. \end{aligned} \quad (46)$$

6.2. Wrong-Sign decays: $\ell \rightarrow \ell' \ell'' \bar{\ell}'''$ with $\ell \neq \ell' = \ell'' \neq \ell'''$

These processes have no penguin contributions, only box diagrams are involved, so the decay width of $\ell \rightarrow \ell' \ell'' \bar{\ell}'''$ is

$$\Gamma(\ell \rightarrow \ell' \ell'' \bar{\ell}''') = \frac{\alpha^2 m_\ell^5}{192\pi} |F_B|^2, \quad (47)$$

the box diagrams are shown in Fig. 4.

The form factor for each box diagram in Fig. 4 is written as follows

$$\begin{aligned} F_B^{\nu_i^l \nu_j^l} &= \frac{\alpha_W}{16\pi M_W^2 s_W^2} \sum_{i,j=1}^3 \{W_{\ell i} W_{\ell' j}^\dagger W_{\ell'' j} W_{\ell''' i}^\dagger \\ &+ (\ell' \leftrightarrow \ell''')\} f_B^l(y_i, y_j), \end{aligned} \quad (48)$$

$$\begin{aligned} F_B^{\nu_i^l \chi_j^h} &= \frac{\alpha_W}{16\pi M_W^2 s_W^2} \sum_{i=1}^3 \sum_{j=7}^9 \{W_{\ell i} W_{\ell' i}^\dagger \theta_{\ell'' j}^\dagger \theta_{\ell''' j} \\ &+ (\ell' \leftrightarrow \ell''')\} f_B^{lh}(y_i, x_j), \end{aligned} \quad (49)$$

$$\begin{aligned} F_B^{\chi_i^h \chi_j^h} &= \frac{\alpha_W}{16\pi M_W^2 s_W^2} \sum_{i,j=7}^9 \{\theta_{\ell i}^\dagger \theta_{\ell' i} \theta_{\ell'' j}^\dagger \theta_{\ell''' j} \\ &+ (\ell' \leftrightarrow \ell''')\} f_B^h(x_i, x_j), \end{aligned} \quad (50)$$

where the y_i and x_i variables are defined in Subsec. 6.1, whose behavior is $x_i, y_j \rightarrow 0$. The f_B^l , f_B^{lh} , and f_B^h functions are Four-point Functions. The ordinary f_B^l function is given by

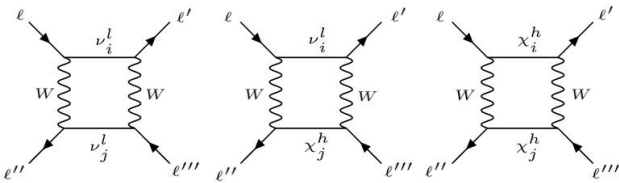


FIGURE 4. Box diagrams, without Majorana neutrino contributions.

$$f_B^l(y_i, y_j) = \left(1 + \frac{1}{4} y_i y_j\right) \bar{d}_0(y_i, y_j) - 2y_i y_j d_0(y_i, y_j), \quad (51)$$

where $\bar{d}_0(y_i, y_j)$ and $d_0(y_i, y_j)$ can be consulted in the Appendix C.3 of [12]. The other functions f_B^{lh} and f_B^h are obtained straightforwardly by doing the corresponding change of variables.

In addition, we have box diagrams with LNV vertices which are shown in Fig. 5. The form factor due to light neutrinos is

$$\begin{aligned} F_{B-LNV}^{\nu_i^l \nu_j^l} &= \frac{\alpha_W}{16\pi M_W^2 s_W^2} \sum_{i,j}^3 W_{\ell i} W_{\ell' j}^\dagger W_{\ell'' i} W_{\ell''' j}^\dagger \\ &\times f_B^{l-LNV}(y_i, y_j). \end{aligned} \quad (52)$$

The contributions from diagrams that mix light and heavy neutrino and diagrams that consider just heavy neutrinos are given by

$$\begin{aligned} F_{B-LNV}^{\nu_i^l \chi_j^h} &= \frac{\alpha_W}{16\pi M_W^2 s_W^2} \sum_{i=1}^3 \sum_{j=7}^9 W_{\ell i} \theta_{\ell' j} W_{\ell'' i} \theta_{\ell''' j} \\ &\times f_B^{lh-LNV}(y_i, x_j), \end{aligned} \quad (53)$$

$$\begin{aligned} F_{B-LNV}^{\chi_i^h \chi_j^h} &= \frac{\alpha_W}{16\pi M_W^2 s_W^2} \sum_{i,j=7}^9 \theta_{\ell i}^\dagger \theta_{\ell' j} \theta_{\ell'' i}^\dagger \theta_{\ell''' j} \\ &\times f_B^{h-LNV}(x_i, x_j). \end{aligned} \quad (54)$$

For the functions $f_B^{(l, lh, h)-LNV}(z_i, z_j)$, we can apply the same arguments as the previous $f_B^{(l, lh, h)}(z_i, z_j)$. Therefore

$$\begin{aligned} f_B^{l-LNV}(y_i, y_j) &= \sqrt{y_i y_j} (2\bar{d}_0(y_i, y_j) \\ &- (4 + y_i y_j) d_0(y_i, y_j)), \end{aligned} \quad (55)$$

for $f_B^{(lh, h)}(z_i, z_j)$ we do the appropriate conversion of variables.

So, the complete form factor reads

$$\begin{aligned} F_B &= F_B^{\nu_i^l \nu_j^l} + F_B^{\nu_i^l \chi_j^h} + F_B^{\chi_i^h \chi_j^h} \\ &+ F_{B-LNV}^{\nu_i^l \nu_j^l} + F_{B-LNV}^{\nu_i^l \chi_j^h} + F_{B-LNV}^{\chi_i^h \chi_j^h}. \end{aligned} \quad (56)$$

After considering some approximations ($x_i, y_i \rightarrow 0$), we obtained that the branching ratio for wrong sign processes is simplified as follows

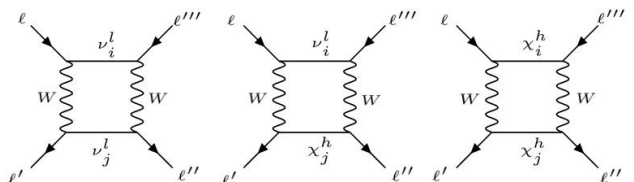


FIGURE 5. Contributions coming from LNV diagrams.

$$\begin{aligned} \text{Br}(\ell \rightarrow \ell' \ell'' \bar{\ell}''') &= \frac{\alpha_W^2}{128\pi^2} \left| -\{\theta_{\ell i} \theta_{\ell' i}^\dagger \theta_{\ell'' j} \theta_{\ell''' j}^\dagger + (\ell' \leftrightarrow \ell'')\} + \{\theta_{\ell i}^\dagger \theta_{\ell' i} \theta_{\ell'' j}^\dagger \theta_{\ell''' j} + (\ell' \leftrightarrow \ell'')\} \left[\left(\frac{1}{2x_j} - 3 \right) \frac{x_i}{2x_j} \ln \left(\frac{x_i}{x_j} \right) \right. \right. \\ &+ \frac{1}{4x_j} \ln \left(\frac{x_i}{x_j} \right) + \frac{1}{4} (6 \ln x_j + 7) \left. \right] + \{\theta_{\ell i}^\dagger \theta_{\ell' j} \theta_{\ell'' i}^\dagger \theta_{\ell''' j}\} \left[\sqrt{\frac{x_i}{x_j}} \ln \left(\frac{x_j}{x_i} \right) + \sqrt{\frac{x_i}{x_j}} (2 \ln x_i + 1) \right. \\ &\left. \left. + \frac{1}{\sqrt{x_i x_j}} (\ln x_j + 1) + \sqrt{\frac{x_j}{x_i}} (2 \ln x_j + 1) \right] \right|^2. \end{aligned} \quad (57)$$

From the expression above we could find values for branching ratios of wrong sign processes which are bound $\text{Br}(\tau \rightarrow ee\bar{\mu}) < 1.5 \times 10^{-8}$ and $\text{Br}(\tau \rightarrow \mu\mu\bar{e}) < 1.7 \times 10^{-8}$ (C.L = 90%) [42].

7. Numerical analysis for wrong sign processes

We study two tau decays known as wrong-sign processes: $\tau \rightarrow ee\bar{\mu}$ and $\tau \rightarrow \mu\mu\bar{e}$. This analysis is done by a Monte Carlo simulation where both processes are computed simultaneously assuming that the LNV couplings are free parameters, thus we are able to bind them. So we have 9 free parameters for each wrong sign processes which will be: the masses of heavy neutrinos, M_i that are the same for both processes and the LNV couplings corresponding to each decay:

- $\tau \rightarrow ee\bar{\mu}$: LNV couplings: $(\theta_{\mu i} \theta_{\tau i})^\dagger$, and $\theta_{ei} \theta_{ei}$ with $i = 1, 2, 3$. We bind the couplings as follows [44]

$$\begin{aligned} |\theta_{\mu 1} \theta_{\tau 1}| + |\theta_{\mu 2} \theta_{\tau 2}| + |\theta_{\mu 3} \theta_{\tau 3}| &< 1.225 \times 10^{-3}, \\ |\theta_{e 1} \theta_{e 1}| + |\theta_{e 2} \theta_{e 2}| + |\theta_{e 3} \theta_{e 3}| &< 0.050, \end{aligned} \quad (58)$$

and their product must satisfy [44]

$$|\theta_{\mu i} \theta_{\tau i}| |\theta_{e j} \theta_{e j}| < 6.125 \times 10^{-5}. \quad (59)$$

TABLE III. Final results. Mean values.

LFV Type III	
$\text{Br}(\tau \rightarrow ee\bar{\mu})$	1.6×10^{-9}
$\text{Br}(\tau \rightarrow \mu\mu\bar{e})$	1.6×10^{-9}
Heavy neutrino masses	
$M_1(\text{TeV})$	3.9
$M_2(\text{TeV})$	3.9
$M_3(\text{TeV})$	3.9
LNV couplings	
$ \theta_{\mu i} \theta_{\tau i} $	2×10^{-3}
$ \theta_{ei} \theta_{ei} $	2×10^{-2}
$ \theta_{ei} \theta_{\tau i} $	9×10^{-4}
$ \theta_{\mu i} \theta_{\mu i} $	4×10^{-2}

- $\tau \rightarrow \mu\mu\bar{e}$: LNV couplings: $(\theta_{ei} \theta_{\tau i})^\dagger$, and $(\theta_{\mu i} \theta_{\mu i})$ with $i = 1, 2, 3$. Bounds on the couplings are [44]

$$\begin{aligned} |\theta_{e 1} \theta_{\tau 1}| + |\theta_{e 2} \theta_{\tau 2}| + |\theta_{e 3} \theta_{\tau 3}| &< 2.704 \times 10^{-3}, \\ |\theta_{\mu 1} \theta_{\mu 1}| + |\theta_{\mu 2} \theta_{\mu 2}| + |\theta_{\mu 3} \theta_{\mu 3}| &< 0.021, \end{aligned} \quad (60)$$

with their product fulfilling [44]

$$|\theta_{ei} \theta_{\tau i}| |\theta_{\mu j} \theta_{\mu j}| < 5.678 \times 10^{-5}. \quad (61)$$

The heavy neutrino masses run from 0.2 to 10 TeVs.

We do not expect large correlations among the two wrong-sign decay modes as they depend on different combinations of theta products. We however check if there is any residual effect induced by their common dependence on the heavy neutrino masses. After doing an analysis of the col-

TABLE IV. Mean values for branching ratios, conversion rates and three heavy neutrino masses (at C.L. = 95% for the Z decays and at 90% for all other processes).

LFV Z decays	
$\text{Br}(Z \rightarrow \bar{\mu}e)$	1.21×10^{-14}
$\text{Br}(Z \rightarrow \bar{\tau}e)$	1.66×10^{-8}
$\text{Br}(Z \rightarrow \bar{\tau}\mu)$	1.13×10^{-8}
LFV Type I	
$\text{Br}(\mu \rightarrow ee\bar{e})$	1.30×10^{-14}
$\text{Br}(\tau \rightarrow ee\bar{e})$	4.08×10^{-9}
$\text{Br}(\tau \rightarrow \mu\mu\bar{\mu})$	4.15×10^{-9}
LFV Type II	
$\text{Br}(\tau \rightarrow e\mu\bar{\mu})$	3.61×10^{-9}
$\text{Br}(\tau \rightarrow \mu e\bar{e})$	2.21×10^{-9}
$\mu - e$ conversion rate	
$\mathcal{R}(\text{Ti})$	5.84×10^{-14}
$\mathcal{R}(\text{Au})$	7.83×10^{-14}
Heavy neutrino masses	
$M_1(\text{TeV})$	4.049
$M_2(\text{TeV})$	4.050
$M_3(\text{TeV})$	4.044

lected data of the Monte Carlo simulation we find that the correlation coefficient between branching ratios is 0.08 which means a practically null correlation.

In the Table III we write down the resulting mean values for each free parameter of this model: three heavy neutrino masses M_i , LNV couplings and the branching ratios for both decays. We conclude that in this model branching ratios corresponding to wrong-sign decays are one order of magnitude below the current upper limits. Thus, there are no sizable correlations among heavy neutrino masses (C.L.=90%).

In Table IV we show the mean values for the other LFV processes which are computed simultaneously with a single Monte Carlo simulation since in contrast to wrong sign processes, they share the same free parameters.

We see that the difference among mean values for the heavy neutrino masses from the previous results in Table III and IV is $\sim 3\%$ in all cases.

8. Lepton number violating tau decays

These processes are represented as follows

$$\tau^-(p_\tau) \rightarrow \ell^+(p_{\ell^+})M_1^-(q_1)M_2^-(q_2), \quad (62)$$

where $M_1^-, M_2^- = \pi, K$.

We consider only tree level amplitude as it is the dominant contribution. Box diagrams are not taken into account. The decay amplitude for lepton number violating tau decays can be separated into leptonic and hadronic parts

$$i\mathcal{M} = (\mathcal{M}_{lep})_{\mu\nu}(\mathcal{M}^{had})^{\mu\nu}, \quad (63)$$

where

$$\begin{aligned} (\mathcal{M}_{lep})_{\mu\nu} &= -\frac{g^2}{2} \sum_{i=1}^3 \bar{v}(p_\tau) \left(\frac{W_{\tau i}^\dagger W_{\ell^+ i}^\dagger m_i}{k^2 - m_i^2} + \frac{\theta_{\tau i} \theta_{\ell^+ i} M_i}{q^2 - M_i^2} \right) \\ &\quad \times \gamma_\mu \gamma_\nu P_R v(p_{\ell^+}), \quad (64) \\ (\mathcal{M}^{had})^{\mu\nu} &= -g^2 V_{M_1}^{CKM} V_{M_2}^{CKM} f_{M_1} f_{M_2} q_1^\mu q_2^\nu \\ &\quad + (M_1 \leftrightarrow M_2), \quad (65) \end{aligned}$$

with m and M the masses of light and heavy Majorana neutrinos, respectively. The leptonic part of the subprocess $\tau^- \rightarrow \ell^+ W^{*-} W^{*-}$ is obtained by crossing the $W^- W^- \rightarrow \ell^- \ell^-$ amplitude.

The total amplitude has two contributions: one comes from light neutrinos (\mathcal{M}_{light}) and the second one comes from heavy neutrinos (\mathcal{M}_{heavy}). The part of light neutrinos is very suppressed due to their masses. Therefore, we work only with heavy neutrinos contribution.

$$\text{Br}(\tau^- \rightarrow e^+ \pi^- \pi^-) < 6.47 \times 10^{-27}, \quad (66)$$

$$\text{Br}(\tau^- \rightarrow \mu^+ \pi^- \pi^-) < 5.88 \times 10^{-27}, \quad (67)$$

$$\text{Br}(\tau^- \rightarrow e^+ K^- K^-) < 1.01 \times 10^{-29}, \quad (68)$$

$$\text{Br}(\tau^- \rightarrow \mu^+ K^- K^-) < 9.19 \times 10^{-30}, \quad (69)$$

$$\text{Br}(\tau^- \rightarrow e^+ \pi^- K^-) < 2.73 \times 10^{-28}, \quad (70)$$

$$\text{Br}(\tau^- \rightarrow \mu^+ \pi^- K^-) < 2.48 \times 10^{-28}. \quad (71)$$

We can see that our results obtained by LHT extended with Majorana neutrinos through ISS are much more constrained than the current limits [42]. This was expected because we started from the fact that \mathcal{M}_{heavy} is small due to the masses of the heavy neutrinos. As heavy neutrino masses are of the order of TeVs there is no resonant enhancement.

9. Conclusions

- LHT is not able to bind LFV processes known as “wrong-sign” through T-odd leptons. However, when we extend the LHT model involving Majorana neutrinos with aid of ISS, the branching ratios get a finite value (C.L. = 90%):

$$\text{Br}(\tau \rightarrow ee\bar{\mu}) < 1.483 \times 10^{-9},$$

$$\text{Br}(\tau \rightarrow \mu\mu\bar{e}) < 1.658 \times 10^{-9},$$

which are one order of magnitude more suppressed than the current values [42].

- LHT extended with Majorana neutrinos also allows us to bind the LNV couplings (C.L. = 90%), which have not been reported before in papers as [44]

$$|\theta_{\mu i} \theta_{\tau i}| < 13.47 \times 10^{-4}, \quad |\theta_{e i} \theta_{e i}| < 2.609 \times 10^{-2},$$

$$|\theta_{e i} \theta_{\tau i}| < 1.413 \times 10^{-3}, \quad |\theta_{\mu i} \theta_{\mu i}| < 2.484 \times 10^{-2}.$$

- The mean values for $\tau \rightarrow \ell\ell'\bar{\ell}'$ decays and $\mu \rightarrow e$ conversion in Ti obtained in our simulation are one order of magnitude smaller than current limits. In $\mu \rightarrow ee\bar{e}$, $Z \rightarrow \bar{\tau}\ell$ and conversion in Au, we get mean values around two orders of magnitude smaller than current limits. Unlike above processes, only $Z \rightarrow \bar{\mu}e$ is not a candidate to be probed in the near future as our result is seven orders of magnitude smaller than current limit.
- Due to heavy Majorana neutrino masses are at order of TeVs, semileptonic three body tau decays are very suppressed. Hence, they are not phenomenological interest as there is no “resonant enhancement”.

1. I. Pacheco, and P. Roig, *Lepton flavor violation in the Littlest Higgs Model with T parity realizing an inverse seesaw*, [arXiv:2110.03711 [hep-ph]].
2. N. Arkani-Hamed, A. G. Cohen and H. Georgi, (De)Constructing Dimensions, *Phys. Rev. Lett.* **86** (2001) 4757, <https://doi.org/10.1103/PhysRevLett.86.4757>
3. N. Arkani-Hamed, A. G. Cohen, E. Katz and A. E. Nelson, The Littlest Higgs, *JHEP* **07** (2002) 034, <https://iopscience.iop.org/article/10.1088/1126-6708/2002/07/034/meta>.
4. M. Schmaltz, D. Tucker-Smith, Little Higgs Review, *Ann. Rev. Nucl. Part. Sci.* **55** (2005) 229, <https://doi.org/10.1146/annurev.nucl.55.090704.151502>
5. Tao Han, Heather E. Logan, Lian-Tao Wang, Smoking-gun signatures of little Higgs models, *JHEP* **01** (2006) 099, <https://doi.org/10.1088/1126-6708/2006/01/099>.
6. M. Perelstein, Little Higgs Models and Their Phenomenology, *Prog. Part. Nucl. Phys.* **58** (2007) 247, <https://doi.org/10.1016/j.pnpnp.2006.04.001>
7. N. Arkani-Hamed, A. G. Cohen and H. Georgi, Electroweak symmetry breaking from dimensional deconstruction, *Phys. Lett. B* **513** (2001) 232, [https://doi.org/10.1016/S0370-2693\(01\)00741-9](https://doi.org/10.1016/S0370-2693(01)00741-9).
8. H. C. Cheng and I. Low, TeV symmetry and the little hierarchy problem, *JHEP* **09** (2003) 051, <https://doi.org/10.1088/1126-6708/2003/09/051>.
9. H. C. Cheng and I. Low, Little hierarchy, little Higgses, and a little symmetry, *JHEP* **08** (2004) 061. <https://doi.org/10.1088/1126-6708/2004/08/061>
10. I. Low, T parity and the littlest Higgs, *JHEP* **10** (2004) 067. <https://doi.org/10.1088/1126-6708/2004/10/067>
11. H. C. Cheng, I. Low and L. T. Wang, Top partners in little Higgs theories with T-parity, *Phys. Rev. D* **74** (2006) 055001. <https://doi.org/10.1103/PhysRevD.74.055001>
12. F. del Aguila, J. I. Illana, and M. D. Jenkins, Precise limits from lepton flavour violating processes on the Littlest Higgs model with T-parity, *JHEP* **01** (2009) 080, <https://doi.org/10.1088/1126-6708/2009/01/080>.
13. J. Reuter, M. Tonini, and M. de Vries, Littlest Higgs with T-parity: Status and Prospects, *JHEP* **1402** (2014) 053, [https://doi.org/10.1007/JHEP02\(2014\)053](https://doi.org/10.1007/JHEP02(2014)053),
14. J. Hubisz, P. Meade, A. Noble, and M. Perelstein, Electroweak Precision Constraints on the Littlest Higgs Model with T Parity, *JHEP* **01** (2006) 135, <https://doi.org/10.1088/1126-6708/2006/01/135>,
15. J. Hubisz and P. Meade, Phenomenology of the littlest Higgs with T-parity, *Phys. Rev. D* **71** (2005), 035016. <https://doi.org/10.1103/PhysRevD.71.035016>
16. J. Hubisz, S. J. Lee and G. Paz, The Flavor of a little Higgs with T-parity, *JHEP* **06** (2006) 041. <https://doi.org/10.1088/1126-6708/2006/06/041>
17. C. R. Chen, K. Tobe and C. P. Yuan, Higgs boson production and decay in little Higgs models with T-parity, *Phys. Lett. B* **640** (2006) 263, <https://doi.org/10.1016/j.physletb.2006.07.053>
18. M. Blanke, A. J. Buras, A. Poschenrieder, C. Tarantino, S. Uhlig and A. Weiler, Particle-Antiparticle Mixing, $\epsilon(K)$, $\Delta\Gamma(q)$, $A^{**}q(SL)$, $A(CP)(B(d) \rightarrow \psi K(S))$, $A(CP)(B(s) \rightarrow \psi \phi)$ and $B \rightarrow X(s,d \gamma)$ in the Littlest Higgs Model with T-Parity, *JHEP* **12** (2006), 003. <https://doi.org/10.1088/1126-6708/2006/12/003>
19. A. J. Buras, A. Poschenrieder, S. Uhlig and W. A. Bardeen, Rare K and B Decays in the Littlest Higgs Model without T^- Parity, *JHEP* **11** (2006), 062. <https://doi.org/10.1088/1126-6708/2006/11/062>
20. A. Belyaev, C. R. Chen, K. Tobe and C. P. Yuan, Phenomenology of littlest Higgs model with T^- parity: including effects of T^- odd fermions, *Phys. Rev. D* **74** (2006) 115020. <https://doi.org/10.1103/PhysRevD.74.115020>
21. M. Blanke *et al.*, Rare and CP-Violating K and B Decays in the Littlest Higgs Model with T^- Parity,” *JHEP* **01** (2007), 066 <https://doi.org/10.1088/1126-6708/2007/01/066>
22. M. Blanke, A. J. Buras, B. Duling, A. Poschenrieder and C. Tarantino, Charged Lepton Flavour Violation and $(g-2)(\mu)$ in the Littlest Higgs Model with T-Parity: A Clear Distinction from Supersymmetry, *JHEP* **05** (2007) 013. <https://doi.org/10.1088/1126-6708/2007/05/013>
23. C. T. Hill and R. J. Hill, T^- Parity Violation by Anomalies, *Phys. Rev. D* **76** (2007), 115014. <https://doi.org/10.1103/PhysRevD.76.115014>
24. T. Goto, Y. Okada and Y. Yamamoto, Ultraviolet divergences of flavor changing amplitudes in the littlest Higgs model with T-parity, *Phys. Lett. B* **670** (2009), 378-382 <https://doi.org/10.1016/j.physletb.2008.11.022>
25. M. Blanke, A. J. Buras, B. Duling, S. Recksiegel and C. Tarantino, FCNC Processes in the Littlest Higgs Model with T-Parity: a 2009 Look, *Acta Phys. Polon. B* **41** (2010), 657-683.
26. F. del Aguila, J. I. Illana and M. D. Jenkins, Muon to electron conversion in the Littlest Higgs model with T-parity, *JHEP* **09** (2010), 040. [https://doi.org/10.1007/JHEP09\(2010\)040](https://doi.org/10.1007/JHEP09(2010)040)
27. T. Goto, Y. Okada and Y. Yamamoto, Tau and muon lepton flavor violations in the littlest Higgs model with T-parity, *Phys. Rev. D* **83** (2011), 053011. <https://doi.org/10.1103/PhysRevD.83.053011>
28. X. F. Han, L. Wang, J. M. Yang and J. Zhu, Little Higgs theory confronted with the LHC Higgs data, *Phys. Rev. D* **87** (2013) 055004. <https://doi.org/10.1103/PhysRevD.87.055004>.
29. B. Yang, N. Liu and J. Han, Top quark flavor-changing neutral-current decay to a 125 GeV Higgs boson in the littlest Higgs model with T parity, *Phys. Rev. D* **89** (2014) 034020. <https://doi.org/10.1103/PhysRevD.89.034020>
30. B. Yang, G. Mi and N. Liu, Higgs couplings and Naturalness in the littlest Higgs model with T-parity at the LHC and TLEP, *JHEP* **10** (2014) 047. [https://doi.org/10.1007/JHEP10\(2014\)047](https://doi.org/10.1007/JHEP10(2014)047).

31. M. Blanke, A. J. Buras and S. Recksiegel, Quark flavour observables in the Littlest Higgs model with T-parity after LHC Run 1, *Eur. Phys. J. C* **76** (2016) 182. <https://doi.org/10.1140/epjc/s10052-016-4019-7>
32. B. Yang, J. Han and N. Liu, Lepton flavor violating Higgs boson decay $h \rightarrow \mu\tau$ in the littlest Higgs model with T parity, *Phys. Rev. D* **95** (2017) 035010. <https://doi.org/10.1103/PhysRevD.95.035010>
33. F. del Aguila *et al.*, Lepton Flavor Changing Higgs decays in the Littlest Higgs Model with T-parity, *JHEP* **08** (2017) 028 [erratum: *JHEP* **02** (2019), 047]. [https://doi.org/10.1007/JHEP08\(2017\)028](https://doi.org/10.1007/JHEP08(2017)028)
34. D. Dercks, G. Moortgat-Pick, J. Reuter and S. Y. Shim, The fate of the Littlest Higgs Model with T-parity under 13 TeV LHC Data, *JHEP* **05** (2018) 049. [https://doi.org/10.1007/JHEP05\(2018\)049](https://doi.org/10.1007/JHEP05(2018)049)
35. F. del Aguila, L. Ametller, J. I. Illana, J. Santiago, P. Talavera and R. Vega-Morales, The full lepton flavor of the littlest Higgs model with T-parity, *JHEP* **07** (2019) 154. [https://doi.org/10.1007/JHEP07\(2019\)154](https://doi.org/10.1007/JHEP07(2019)154)
36. F. Del Aguila, J. I. Illana, J. M. Pérez-Poyatos and J. Santiago, Inverse see-saw neutrino masses in the Littlest Higgs model with T-parity, *JHEP* **12** (2019) 154. [https://doi.org/10.1007/JHEP12\(2019\)154](https://doi.org/10.1007/JHEP12(2019)154)
37. J. I. Illana and J. M. Pérez-Poyatos, A new and gauge-invariant Littlest Higgs model with T-parity, [arXiv:2103.17078[hep-ph]]
38. A. Ilakovac and A. Pilaftsis, Flavor violating charged lepton decays in seesaw-type models, *Nucl. Phys. B* **437** (1995) 491, [https://doi.org/10.1016/0550-3213\(94\)00567-X](https://doi.org/10.1016/0550-3213(94)00567-X).
39. J. I. Illana and T. Riemann, Charged lepton flavor violation from massive neutrinos in Z decays, *Phys. Rev. D* **63** (2001) 053004, <https://doi.org/10.1103/PhysRevD.63.053004>
40. G. Hernández-Tomé, J. I. Illana, M. Masip, G. López Castro and P. Roig, Effects of heavy Majorana neutrinos on lepton flavor violating processes, *Phys. Rev. D* **101** (2020) 075020, <https://doi.org/10.1103/PhysRevD.101.075020>
41. H. H. Patel, Package-X: A Mathematica package for the analytic calculation of one-loop integrals, *Comput. Phys. Commun.* **197** (2015) 276, <https://doi.org/10.1016/j.cpc.2015.08.017>
42. P. A. Zyla *et al.*, Review of Particle Physics, *PTEP* **2020** (2020) 083C01. <https://doi.org/10.1093/ptep/ptaa104>.
43. A. Abdesselam *et al.*, Search for lepton-flavor-violating tau decays to $\ell\gamma$ modes at Belle, *JHEP* **10** (2021) 019, [https://doi.org/10.1007/JHEP10\(2021\)019](https://doi.org/10.1007/JHEP10(2021)019).
44. E. Fernández-Martínez, J. Hernández-García and J. López-Pavón, Global constraints on heavy neutrino mixing, *JHEP* **08** (2016) 033, [https://doi.org/10.1007/JHEP08\(2016\)033](https://doi.org/10.1007/JHEP08(2016)033)